



Calorimetric and physico-chemical study of sulfobetaines micellization in the presence and the absence of polystyrene nanoparticles.

Fatima Yssaad¹, Teffaha Fergoug¹, Meriem Dadouch^{1,2}, Rachida Aribi¹, Fatima Zohra Chater¹, Aicha Kadiri¹, Youcef Bouhadda^{1,*}

¹Laboratory of Physical chemistry of macromolecules and biological interfaces, Mustapha Stambouli university, Mascara, 29000, Algeria

²Department of Pharmacy, Faculty of Medicine, Djillali Liabes University, Sidi Bel Abbes, 22000, Algeria

ARTICLE INFO

Article history:

Received 3 January 2025

Received in revised form 7 February 2025

Accepted 3 March 2025

Available online 20 March 2025

Keywords:

Sulfobetaines

Micellization

Aggregation number

Polystyrene nanoparticles

Dynamic light scattering

Isothermal titration calorimetry

ABSTRACT

This work investigates thermodynamic and physico-chemical properties of two zwitterionic surfactants (n-alkyl-N, N-dimethyl-3-ammoniopropanesulfonate, SB3-12 and SB3-14) in the presence and absence of polystyrene nanoparticles PS-NPs. The micellization process in water was studied using isothermal titration calorimetry (ITC) and dynamic light scattering (DLS) in the temperature range from 293.15 K to 323.15 K as well as by tensiometry at 298.15 K. For pure surfactant solutions, the increase in both temperature and the alkyl chain length leads to more negative values of Gibbs free energy of micellization (ΔG°_{mic}), favoring the micellization. From the temperature dependence of micellization enthalpy (ΔH°_{mic}), the values of micellization heat capacity changes ($\Delta C^{\circ}_{p, mic}$) were found negative for the two surfactants relating to the removal of water accessible non-polar surfaces. DLS measurements showed that micelles aggregates size D_h are around 5.5 nm and 6.5 nm for SB3-12 and SB3-14 respectively with a pronounced hydrophobic effect as confirmed from tensiometry experiments. Furthermore, the aggregation numbers N_{agg} of SB3-12 and SB3-14 micelles were determined from isothermal titration calorimetry for the first time. The deduced values were in agreement with (DLS) results at high temperatures. In the presence of polystyrene nanoparticles (PS-NPs), the formation of micellar aggregates occurs by association between PS-NPs and surfactants at low concentration of surfactants as revealed from ITC and DLS analysis. These results suggest that the PS-NPs/surfactant association is based on hydrophobic interactions.

1. Introduction

The combination of polymers and surfactants to formulate new nano-like particles represents a highly compelling area of research within materials science, with numerous applications in drug delivery, oil recovery, cosmetics, wastewater treatment, and the remediation of contaminated soils [1-4]. However, prior to their application, this advantageous pairing must undergo a series of tests to assess their compatibility and behavior under various thermodynamic conditions. The interactions between these components can significantly modify the inherent properties of each individual substance,

potentially resulting in a useless product. In particular, the interaction of surfactants with the polymer's hydrocarbon chains can affect its conformation, charge, and size, leading to various undesired outcomes such as expansion, self-folding, or, in more detrimental cases, self-association and flocculation [5]. Likewise, the polymer may also influence the colloidal characteristics of the surfactant, causing changes in parameters such as critical micellization concentration (cmc), Krafft temperature, or cloud point [6]. Consequently, the polymer-surfactant association can trigger the micellization process prematurely, enhancing the surfactant micelles' detergency. The interaction

* Corresponding author; e-mail: y.bouhadda@univ-mascara.dz

<https://doi.org/10.22034/crl.2025.497364.1517>



This work is licensed under Creative Commons license CC-BY 4.0

between surfactants and polymers is a complex phenomenon. It is widely recognized that the surfactant-polymer interaction arises from a combination of various forces, primarily hydrophobic effects, electrostatic interactions, and hydrogen bonding [7] which induce either the binding of surfactant monomers to the polymer chain or the micellization of surfactants near the polymer chain entanglement [8]. Consequently, the thermodynamic model employed to characterize this process must be adapted to reflect the specific type of interaction involved. Numerous scientific studies [9, 10] that address the combination of polymers and surfactants exist in the literature. However, there is a notable research gap that inspect this interaction from a thermodynamic perspective for zwitterionic surfactants [11].

In this regard, isothermal titration calorimetry (ITC) emerges as a powerful method for the thermodynamic characterization of physico-chemical phenomena. It is widely recognized that a single ITC experiment conducted for surfactants at a specific temperature can yield simultaneously the critical micelle concentration (cmc) and the standard enthalpy change of micellization (ΔH°_{mic}) [8]. Furthermore, by monitoring the micellization process across various temperatures, several micellization thermodynamic parameters can be determined such as the standard Gibbs free energy change (ΔG°_{mic}), the standard entropy change (ΔS°_{mic}), and the standard heat capacity change ($\Delta C^{\circ}_{p, mic}$), which help to identify the primary forces governing these phenomena [12-13,14]. ITC is also suitable for the thermodynamic analysis of surfactant adsorption onto polymer nanoparticles at varying temperatures and surfactant concentrations. This technique allows the determination of the critical aggregation concentration (cac) of the polymer-surfactant system to indicate the concentration at which interactions between the polymer and surfactant occur [11]. Besides these informations, it is important to consider the size and surface charge of the polymer during these interactions under different experimental conditions. To achieve this, dynamic light scattering (DLS) serves as an effective technique for exploring changes in hydrodynamic diameter D_h [15] and zeta potential of the polymer nanoparticles in the presence of the surfactants. Such information is vital, as excessive swelling of the polymer nanoparticles can alter the rheological properties of the solution, while low zeta potential values may indicate potential instability [16]. This study aims to characterize two zwitterionic surfactants, SB3-12 and SB3-14 (Fig. 1), and their interactions with polystyrene nanoparticles (PS-NPs) using ITC, DLS, and tensiometry. Various thermodynamic (ΔG°_{mic} , ΔS°_{mic} , and $\Delta C^{\circ}_{p, mic}$) as well as physico-chemical

properties (cmc, N_{agg} , D_h) will be examined under different temperatures and surfactant concentrations.

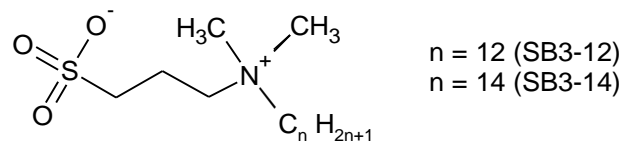


Fig. 1. Chemical structures of the studied zwitterionic surfactants

2. Materials and methods

The zwitterionic surfactants SB3-12 and SB3-14 (>99%) were supplied by Sigma Company and were used without further purification. The polystyrene sample used was provided by Malvern Panalytical, as an aqueous solution with highly uniform polystyrene spheres calibrated by NIST-traceable standards with a nominal diameter of 220 nm and zeta potential of -45 mV. All solutions were freshly prepared with demineralised and de-ionized water, with a conductivity of $6.7\mu\text{S}/\text{cm}$ and a surface tension of 69 mN/m at 298.15 K.

Surface tension measurements

Surface tension (γ) was measured using a Du Noui-type tensiometer (Lauda scientific TC1). It consists of a platinum ring suspended by a wire from a pulley-like device that progressively exerts a vertical force required to pull the ring immersed in the solution, thus allowing the measurement of γ varying from 0 to 90 mN/m with an accuracy of 0.05 mN/m, after calibration of the device.

DLS measurements

The dynamic light scattering (DLS) experiments were performed to measure average size of micelles and PS-NPs using Malvern Zetasizer Instrument Nano-ZS 4800, UK equipped with He-Ne laser operating at a wavelength of 633 nm and a fixed scattering angle of 173° . Each measurement was repeated 3 times and average values were considered. The time dependent correlation function was measured at different temperatures for different concentrations of surfactants above their respective cmc in water in presence and absence of Polystyrene polymer. Analyses were performed in cumulative mode using the integrated Zetasizer software. The correlation function contains the diffusion coefficient information required to be entered into the Stokes-Einstein equation [17] eq.1.

$$D = \frac{K_B T}{3\pi\eta D_h} \quad \text{eq. 1}$$

where, K_B and T stand for Boltzmann constant and absolute temperature respectively. Whereas, D and D_h represent the Diffusion coefficient and the hydrodynamic diameter of the scattering particle in a solvent of viscosity η , respectively.

ITC measurements

The calorimetric measurements were carried out using a TA instruments low-volume Nano ITC calorimeter which enables to measure dilution enthalpies Q_{inj} at different temperatures. A calibration of the ITC was carried out electrically by using electrically generated heat pulses. Furthermore, a CaCl_2 -EDTA titration was performed to check the apparatus, and the results (n-stoichiometry, K, ΔH) were compared with supplier specifications.

Prior to the titration process, samples and used water were degassed and thermostated using an accessory (Vibrating degasser). The homogeneity and the purity of stock solutions of the different surfactants were checked using a sonicator and a tensiometer respectively.

For ITC experiments, 250 μL of each solution with a concentration ten times greater than the cmc were injected sequentially by a computer-controlled syringe (5 μL in each injection) into a 1.30 ml reaction cell containing purified water or polymer water solution. The solution in the reaction cell was agitated at a speed of 250 rpm throughout the experiments and an interval of 400 s between each successive injection was maintained.

After each injection, the computer records the heating rate required Q_{inj} to maintain a constant temperature difference between the sample cell and the reference cell filled with purified water. The change in dilution enthalpy,

ΔH_{dil} , is obtained by dividing Q_{inj} by the number of moles of surfactant injected into each 5 μL aliquot.

For the dilution of micelles in ITC the constitutive equation is given by eq.2 [18]:

$$dQ_{inj} = V \cdot \Delta H^{\circ}_{demic} \cdot d\varepsilon(S_{tot}) \quad \text{eq. 2}$$

where dQ , ΔH°_{demic} and $d\varepsilon$ represent respectively the differential heat, the enthalpy of demicellization estimated by D/STAIN program [12] and the differential extent of reaction respectively. V is the volume of the reaction cell whereas S_{tot} is the total concentration

3. Data treatment

During ITC experiments for surfactant micellisation phenomenon, Time-dependent heat flow curve (Fig 2.a) and sigmoidal curve (Fig 2.b) are obtained and can be divided into three steps [13,19]:

1. Dissociation of micelles into monomers: The generated heat corresponds to the dilution enthalpy of monomers and the titration ITC curve is composed of exothermic peaks.
2. Micellization of the surfactant: The heat generated during this process corresponds to the enthalpy of micellization ΔH°_{mic} .

Micelles dilution: The heat generated during this process corresponds to the micelle dilution enthalpy. In this part, the titration ITC curve is always composed of low and endothermic peaks.

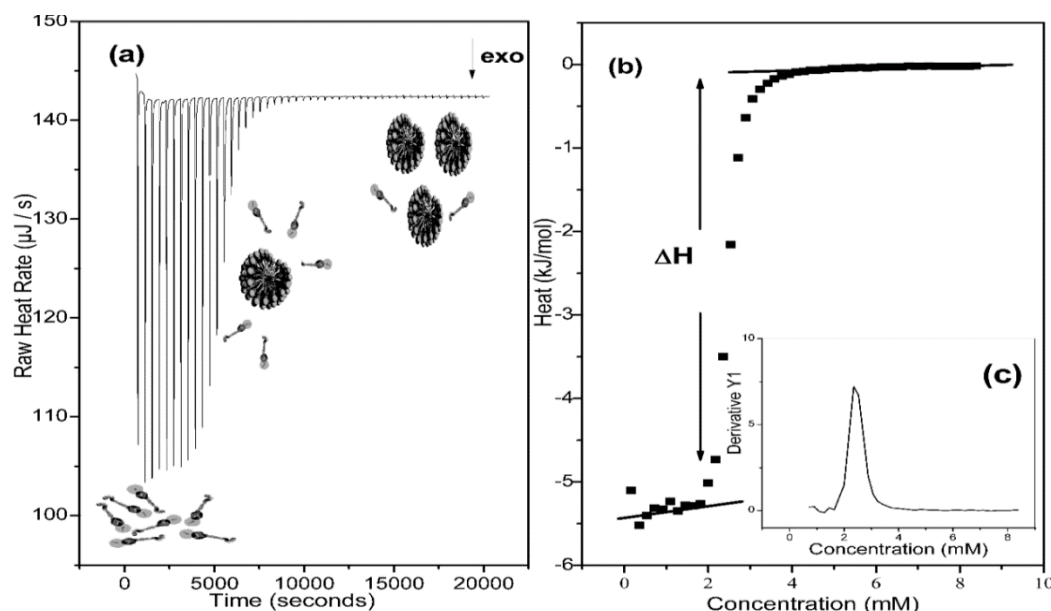


Fig. 2. Titration of micellar solution in the calorimetric cell containing water.

(a) Time-dependent heat flow for 50 injections of 5 μL surfactant in degassed water. (b) the change in heat corresponding to each injection depressing the final concentration. (c) First derivative of the curve in (b) where the maximum corresponds to the cmc.

Thermodynamic parameters extraction

When the solution of surfactants is titrated in water, the ITC records the differential enthalpy variations associated with demicellization and dilution of surfactant molecules. A typical illustration of the heat flow and the corresponding differential graph against the injections for the micellization of a given surfactant in water at 293.15 K is shown in the Fig. 2. In order to get the values of ΔH_{mic}° two steps must be performed. First, we need to extrapolate the pre-micellar (initial) and post-micellar (final) data using linear adjustments (Fig. 2.b). The difference between (initial) and (final) fitting lines, makes it possible to determine ΔH_{obs} [8] which is given by the following expression:

$$\Delta H_{obs} = \Delta H_{dil}(finale) - \Delta H_{dil}(initiale) \quad eq. 3$$

The heat observed is therefore related to a demicellization process, which is the same as the micellization process but with an opposite sign. Thus, the value of the enthalpy of micellization is written :

$$\Delta H_{mic}^{\circ} = -\Delta H_{demic}^{\circ} = \Delta H_{obs} \cdot \frac{C_T}{C_T - cmc} \quad eq. 4$$

The total concentration of surfactant (C_T) in the syringe is much higher than the cmc. In addition, the calculation of the first derivative of the ITC curve (Fig. 2.c) related to the total concentration of surfactant in the cell makes it possible to determine cmc.

According to the pseudo-phase-separation model, the micelles are considered as a separate phase [20]. The standard energy of micellization is given by:

$$\Delta G_{mic}^{\circ} = RT \ln X_{cmc} \quad eq. 5$$

Where X_{cmc} is the molar fraction of the monomers at cmc, R is gas constant and T is temperature. The entropy term can then be derived using the Gibbs- Helmholtz relation:

$$T \Delta S_{mic}^{\circ} = \Delta H_{mic}^{\circ} - \Delta G_{mic}^{\circ} \quad eq. 6$$

The combination of ITC experiments at different temperatures allowed the determination of changes in thermal capacity ($\Delta C_{p, mic}$), according to the following equation:

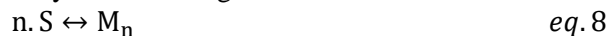
$$\Delta C_{p, mic}^{\circ} = \left(\frac{\partial \Delta H_{mic}^{\circ}}{\partial T} \right)_p \quad eq. 7$$

$\Delta C_{p, mic}^{\circ}$ is an important parameter for the evaluation of hydrophobic contributions [14, 21].

Micelle Aggregation number extraction

Olesen *et al*, proposed a method for extracting N_{agg} from ITC data for a series of 6 bile salts and SDS [22, 18]. They have described an accurate approach of modelling the curves using the mass action law model. Their model considers that at cmc only unimers and surfactant micelles are in equilibrium in the presence of a large amount of

counter ions. In the present work, we use this-model to extract N_{agg} for the zwitterionic surfactants SB3-12 and Sb3-14 that are electrically neutral such that the self-association (micellization) equilibrium between n (number of monomers) and the concentration of a surfactant (S) is given by the following relation:



where S represents the monomeric surfactant and M_n the n-meric micelles.

They are assumed populated at equilibrium, implying that micellization constant is sufficient to describe the equilibrium of the process.

$$K = \frac{M_n}{[S]^n} \quad eq. 9$$

For the model statement, the two-state reaction (Eq. 2), the binding isotherm is written as

$$\frac{dQ}{dS_{tot}} = \Delta H_{demic}^{\circ} V \frac{dS}{dS_{tot}} \quad eq. 10$$

Defining the micellization constant (Eq. 3) and applying the principle of mass conservation

$$S_{tot} = [S] + nK[S]^n \quad eq. 11$$

We obtain an expression with n as the single unknown quantity:

$$\frac{d \ln \left(\left(\frac{d[S]}{dS_{tot}} \right)^{-1} - 1 \right)}{d \ln S_{tot}} = \frac{n-1}{n} + \frac{(n-1)^2}{n} \frac{d[S]}{dS_{tot}} \quad eq. 12$$

The aggregation number can be determined by plotting $\frac{d \ln \left(\left(\frac{d[S]}{dS_{tot}} \right)^{-1} - 1 \right)}{d \ln S_{tot}}$ against $\frac{d[S]}{dS_{tot}}$. This scheme estimates the aggregation number in a fast and reliable way independently of the other parameters. With the aggregation number in hand, the micellization constant can be derived through Eq. 10 from the same ITC experiment by measuring the cmc [23].

4. Results and discussion

Tensiometry results

Fig. 3 shows the variation of surface tension γ against SB3-12 and SB3-14 surfactants concentration at 298.15 K respectively. We note that both molecules exhibit an appreciable surface activity at the water/air interface. By increasing concentration, the surface tension decreases uniformly and reaches a plateau ($\gamma = \gamma_{min}$) from a certain concentration that coincides with the cmc indicating the beginning of micellization [24]. This concentration is determined by the intersection point of two lines obtained by linear regressions of each part of the curve. SB3-14 surfactant (cmc = 0.27 mM and $\gamma_{min} = 34.1$ mN/m) should be more hydrophobic than SB3-12 ones (cmc = 3.2 mM and $\gamma_{min} = 35.2$ mN/m) at 298.15 K.

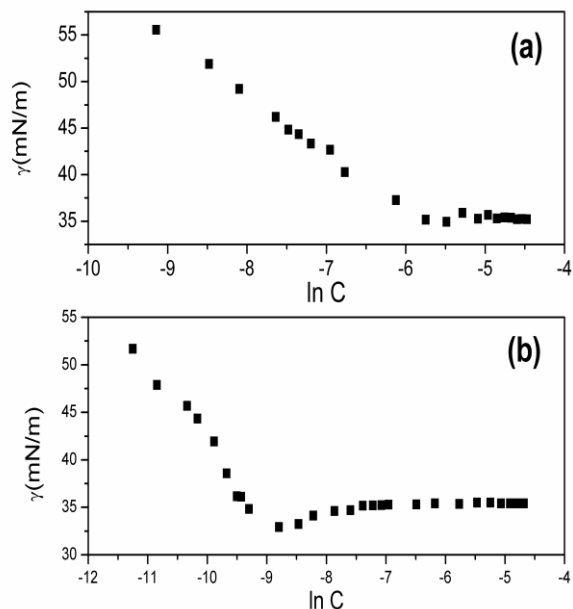


Fig. 3. Variation of the surface tension of SB3-12 (a) and SB3-14 (b) as a function of the concentration at 298.15 K

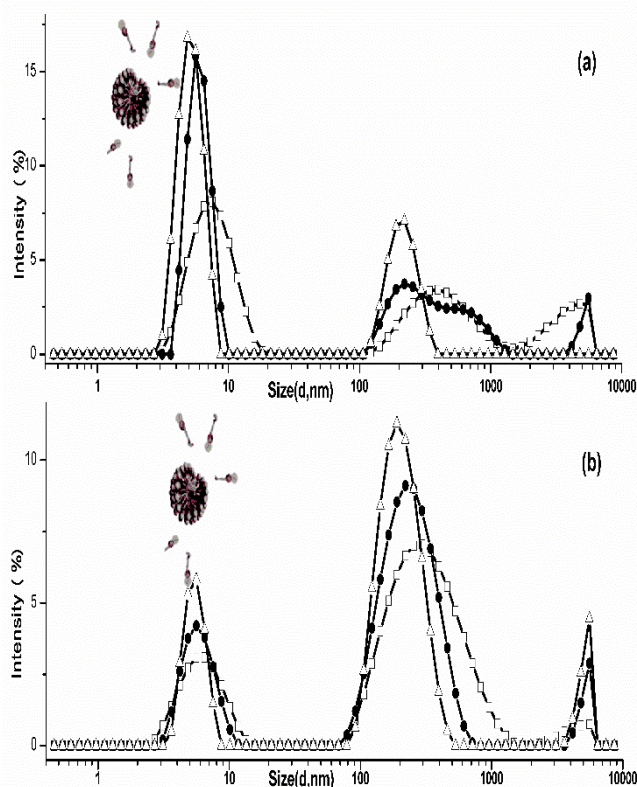


Fig. 4. Temperature effect on hydrodynamic diameter of SB3-12(a) and SB3-14(b) at 293.15 K (\square), 308.15 K (\bullet) and 323.15 K (Δ).

DLS results

Temperature effect

Fig. 4 shows the size distribution by percent intensity at different temperatures for SB3-12 and SB3-14 at $C = 50$ mM and $C = 6$ mM respectively (far from their corresponding cmc inferred from the analysis of the tensiometry data). Firstly, every distribution exhibits a multi-peak feature where the first peaks around 10 nm represent the hydrodynamic diameter of the assumed classical Hartley-type micelles. The fact that SB3-14 micelles are larger than the SB3-12 ones is expected since the former surfactant hydrocarbon chain contains two more carbon atoms.

The others remaining peaks in Fig. 4, result from the association of monomers/micelles species with two types of water-structured clusters (low density level clusters LDL (> 100 nm) and high density ones HDL (> 100 nm)) as presented by Mirgorod *et al.*, and Kadiri *et al* [15, 25] for some model aqueous ionic surfactant solutions.

It is interesting to note that for SB3-12 surfactant the peak width of surfactant/water clusters decreases significantly when temperature increases, whereas for SB3-14 surfactant the corresponding peaks seem to be slightly affected. This behavior difference means that the two surfactants interact differently with the surrounding water molecules despite that they possess the same ionic head and almost the same hydrocarbon chain type. It is well known that the increase in temperature is always accompanied by a process of dehydration of micelles and the hydrated free surfactant molecules, which imposes a rearrangement of micelles into more compact structures with reduced hydrodynamic diameter. Given the tensiometric results which suggest that the two surfactants differ on their hydrophobic character, the variation of the aggregates size under thermal treatment can be explained by the hydration/dehydration argument as will be confirmed below from ITC analysis. Indeed, the hydrophobic effect can be split into two energetic components: the enthalpic hydrophobic effect and the entropic hydrophobic effect, the former is related to expelled water molecules from the hydrophobic surfaces and the latter to the disordered water molecules released after the aggregation process. However, for the micelles peaks below 10 nm the peaks width are relatively slimly influenced by temperature increase as usually reported for aggregates of surfactants [26] but the peaks position shift to lower values (centred on 5 nm for SB3-12 and 6 nm for SB3-14). The obtained value for SB3-14 surfactants is higher than the reported value by Di Profio P *et al* [27] (2.9 nm at 298.15 K at a concentration near cmc). This difference is reasonable since it is well known that the particle size increases with increasing surfactant concentration.

Concentration Effect

Fig. 5 shows the variation of hydrodynamic diameter against SB3-12 and SB3-14 concentration at 298.15 K respectively.

It is widely recognized that no measurable dynamic light scattering (DLS) signal is detected under cmc as micelles are not formed. However, once the concentration surpasses the cmc, a signal becomes evident, allowing for the determination of the hydrodynamic diameter of the resulting micelles. In the case of the two surfactant solutions, the micelle size remains relatively stable or experiences a slight increase (SB3-12) within the concentration range of analyses. The cmc values are approximately 5 mM for SB3-12 and 0.4 mM for SB3-14 surfactants. It is important to highlight that these cmc values differ from those obtained through tensiometry. Such discrepancies arise because the micellization process detectable by tensiometry occurs just beyond the surface adsorption process.

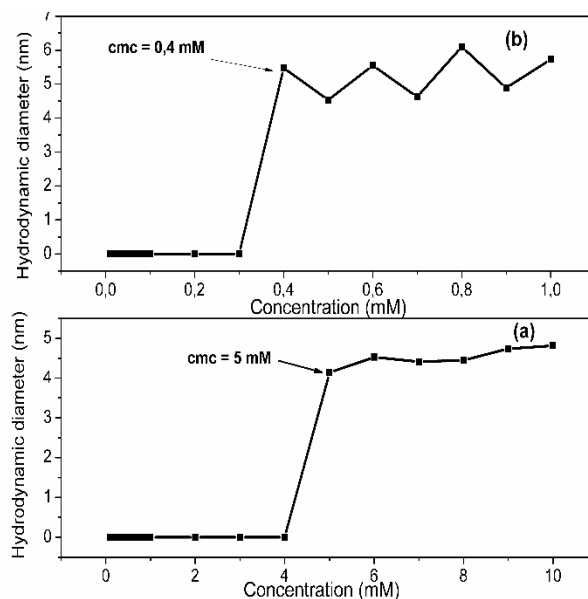


Fig. 5. Effect of concentration on hydrodynamic diameter of surfactant SB3-12 (a) and SB3-14 (b) as a function of concentration at 298.15 K.

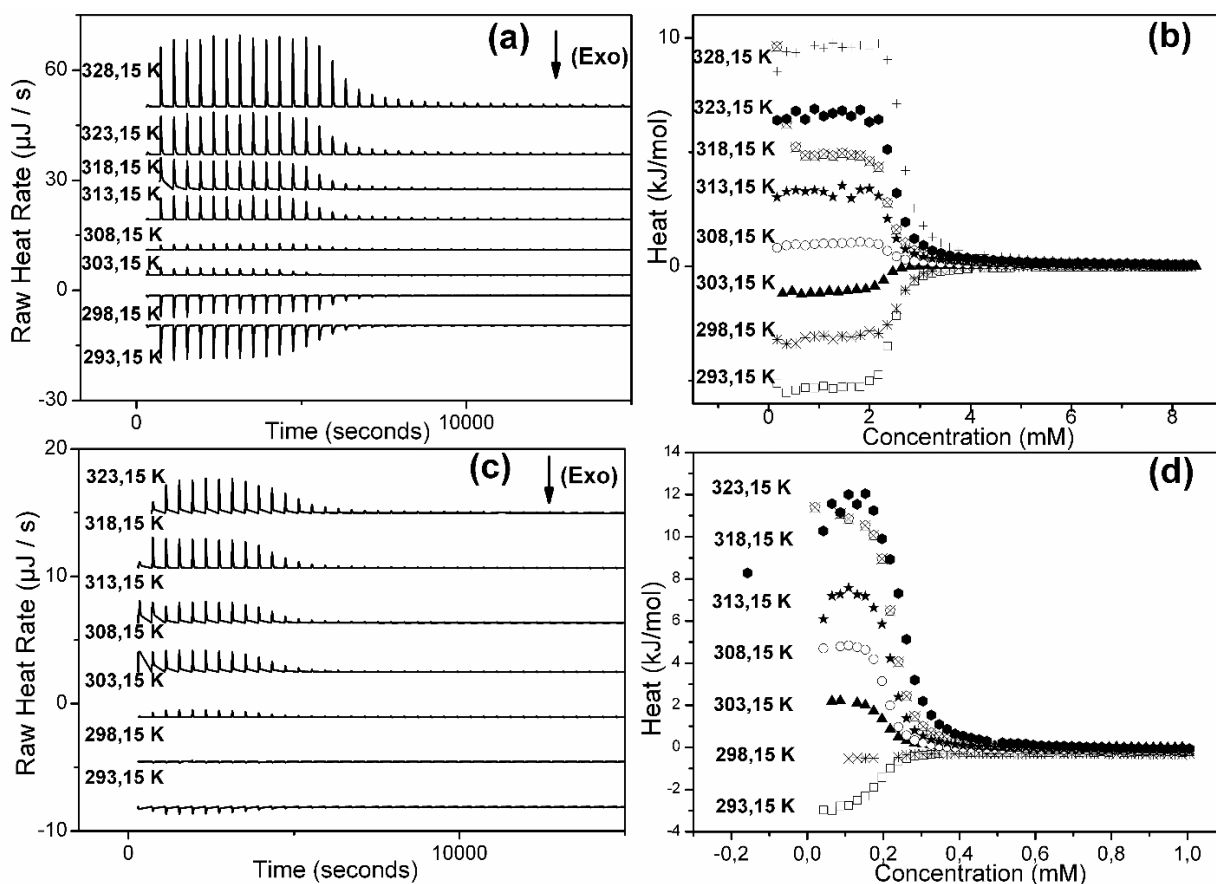


Fig. 6 Titration of micellar solution SB3-12 (50 mM) and SB3-14 (6 mM) in the calorimetric cell (1.3 ml) containing water at different temperatures. (a-c) Time-dependent heat flow for 50 injections of 5 μ L SB3-12 and SB3-14 in degassed water. (b-d) the change in heat corresponding to each injection depressing the final concentration of SB3-12 and SB3-14.

ITC results

Fig. 6 shows the calorimetric titration curves for the micellization of sulfobetaine surfactants SB 3-12, SB3-14 from 293.15 to 323.15 K. The enthalpy change versus SB3-n surfactant concentration curves presented similar profiles at all temperatures: they were highly endothermic up to a particular concentration (cmc) and then became progressively less endothermic above this value. The high endothermic enthalpy observed at lower surfactant concentrations is associated with the breakdown of the SB3-n micelles after they are titrated into the reaction cell because the total surfactant concentration is below the cmc. The progressive decrease of the endothermic enthalpy change above a particular surfactant concentration (cmc) is due to exceeding cmc so that any additional SB3-n micelles added no longer break down. The magnitude of endothermic enthalpy change associated with micelle breakdown, as well as the value of the cmc, depended on the temperature. Micelle breakdown became more endothermic with increasing temperature. This phenomenon can be attributed to the association of enthalpy change with the transfer of a hydrophobic substance from a hydrophobic environment into water becomes increasingly endothermic as temperature increase [28].

The cmcs of the SB3-12 and SB3-14 were determined at several temperatures by determining the inflection point from the enthalpy versus surfactant concentration profiles. As shown on table 1, cmc decreases as the temperature rises until a minimum point is reached ($\text{cmc}_{\min \text{SB3-12}} = 2.34$

mM, $\text{cmc}_{\min \text{SB3-14}} = 0.19$ mM) at a critical temperature T_c and then increases with temperature. It is well known that the effect of temperature on cmc values of surfactants in aqueous solution is due to two opposing phenomenons [29]. The temperature increase reduces the hydration degree of the hydrophilic head group, which favours the micelle formation and decreases the cmc values of surfactants (phenomenon 1). Meanwhile, as the temperature increases the order structure of water molecules neighboring the hydrophobic domain can be broken, which is unfavorable to micellization (phenomenon 2). Thus, it is possible that at lower temperatures, the phenomenon 2 is predominant and above T_c the phenomenon 1 becomes a major effect. As can be seen from Fig. 6, the T_c value for SB3-12 is about 303.15 K, which is higher than that of SB3-14 (T_c is close to 298.15 K). It was reported that T_c is directly dependent on the hydrophobicity of surfactants.

This hypothesis is confirmed by the ITC curves features. In fact, for SB3-12, the ITC curves are sorted as type A curves at all temperatures. This means that the surfactants behave ideally and do not display solute-solute interactions [30]. In this case, the values of the dilution enthalpy (ΔH_{dil}) at the first injections appear identical and constant. However, the ITC curves of SB3-14 are of type B [30]. A high value of ΔH_{dil} at the first injections reveals a non-ideal behavior of the solution. This means that not only interactions between surfactant molecules and water exist, but also interactions between the surfactants themselves which contribute to the observed heat flow variation [31].

Table 1. cmcs and thermodynamic parameters of micellization of zwitterionic surfactants

SB3-12						
T (K)	cmc (mM)	$\Delta H^{\circ}_{\text{mic}}$ (KJ/mol)	$\Delta G^{\circ}_{\text{mic}}$ (KJ/mol)	$\Delta S^{\circ}_{\text{mic}}$ (J/mol.K)	$\Delta C^{\circ}_{\text{p,mic}}$ (J/mol.K)	T_c (K)
293.15	2.470	5.40	-24.42	101.7		
298.15	2.600	3.13	-24.71	93.4		
303.15	2.340	1.11	-25.39	87.4		
308.15	2.400	-1.04	-25.74	80.2		
313.15	2.420	-3.20	-26.14	73.3		
318.15	2.430	-4.30	-26.55	70.0	-432.21	306.15
323.15	2.500	-6.90	-26.89	61.9		
328.15	2.650	-9.80	-27.14	52.9		
SB3-14						
293.15	0.192	2.60	-30.65	113.4		
298.15	0.250	0.27	-30.50	103.4		
303.15	0.196	-2.60	-31.64	95.8		
308.15	0.207	-5.30	-32.02	86.7		
313.15	0.211	-9.30	-32.49	74.0		
318.15	0.228	-10.8	-32.81	69.0	-530.1	298.15
323.15	0.233	-14.9	-33.26	57.0		

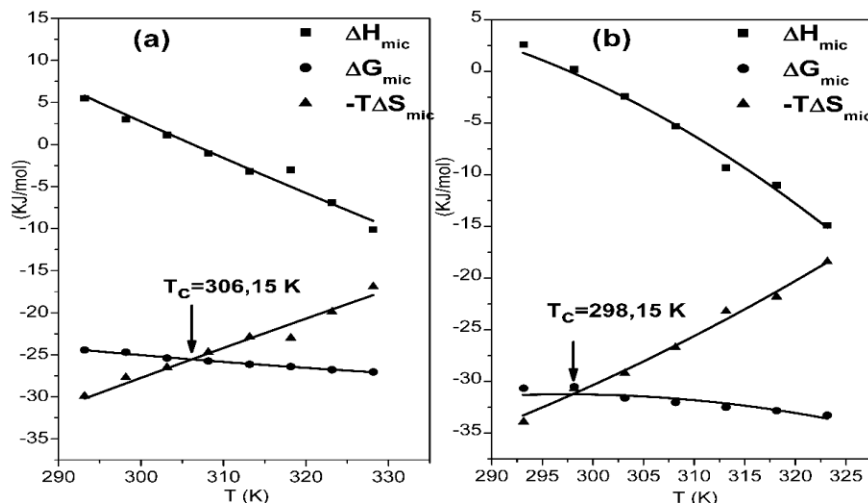


Fig. 7. Thermodynamic parameters for micellization of (a) SB3-12 and (b) SB3-14 as a function of temperature. The intersection of the second polynomial approximation of ΔG°_{mic} and $-T\Delta S^{\circ}_{mic}$ as a function of temperature gives the compensation temperature, T_c

Furthermore, it can be clearly inferred that an increase in hydrophobic alkyl chain length follows the well-known trend, i. e., their cmc values are reduced by an approximate factor of 10 when two methylene groups extend the alkyl chain and these values are in good agreement with ones found by Brinatti *et al* [11]. Once, ΔH°_{mic} and cmc were determined, ΔG°_{mic} and ΔS°_{mic} were deduced using equation 5 and 6, respectively.

Analysis of the experimental values from the phase separation model gives the thermodynamic quantities shown in Table 1.

It can be clearly deduced that the micellization process of the two zwitterionic surfactants is endothermic at low temperatures and becomes exothermic at high ones for all investigated solutions (Fig. 5). A similar change in the sign of ΔH°_{mic} with increasing temperature has been already observed for number of ionic surfactants [32]. As expected and observed previously [24], the ΔG°_{mic} is negative over the whole studied temperature range (Table 1), which means that is thermodynamically favorable and occurs spontaneously.

At low temperatures, the enthalpy contribution to Gibbs' energy is low relative to the entropy term ΔS°_{mic} . However, as the temperature increases, the ΔH°_{mic} becomes more negative and its contribution to ΔG°_{mic} increases. For its part, the ΔS°_{mic} is positive and decreases at high temperature. Thus, its contribution to ΔG°_{mic} also decreases [19, 11].

Enthalpy-Entropy compensation

Fig. 7 shows the temperature dependence of ΔG°_{mic} , ΔH°_{mic} , and $-T\Delta S^{\circ}_{mic}$ for SB3-12 and SB3-14 surfactants in

aqueous solutions. The first derivative of ΔH°_{mic} against temperature at constant pressure yields the heat capacity variation $\Delta C^{\circ}_{p,mic}$ which can be positive when hydrophobic interactions are broken during micellization or negative if hydrophobic interactions are formed [33]. The $\Delta C^{\circ}_{p,mic}$ values obtained for SB3-12 and SB3-14 are -432.21 J/mol.K and -530.1 J/mol.K respectively which means that hydrophobic molecules are transferred from water to a non-polar medium. Furthermore, it can be seen in Fig. 7 that ΔH°_{mic} exhibits a linear dependence on temperature, so $\Delta C^{\circ}_{p,mic}$, is assumed to be constant over the investigated temperature range. In this case, according to E. Sikorska *et al.* [34] the linear behavior of $\Delta C^{\circ}_{p,mic}$ along the temperature range reveals a non-exposed hydrophobic surface in micelle to water. In general, ΔH°_{mic} plots as a function of $-T\Delta S^{\circ}_{mic}$ show a linear relationship, indicating that these thermodynamic parameters are complementary to each other [35, 36]. In Fig.7, the complementarity between ΔH°_{mic} plot and $T\Delta S^{\circ}_{mic}$ one is obvious in agreement with numerous reports showing the existence of enthalpy-entropy compensation for adsorption and micellization of surfactants [37]. It is thought that compensation effect is the consequence of two processes:

- 1) Dehydration process by destruction of the iceberg-shaped structures around the alkyl chains.
- 2) Micelles formation by surfactant alkyl chains aggregation.

Once enthalpy-entropy compensation effect is identified, T_c temperatures at which the process is entropic are derived from the intersection of the second polynomial approximation of temperature dependence of the terms (the thermodynamic functions) ΔG°_{mic} and $-T\Delta S^{\circ}_{mic}$ as shown in Fig. 7.

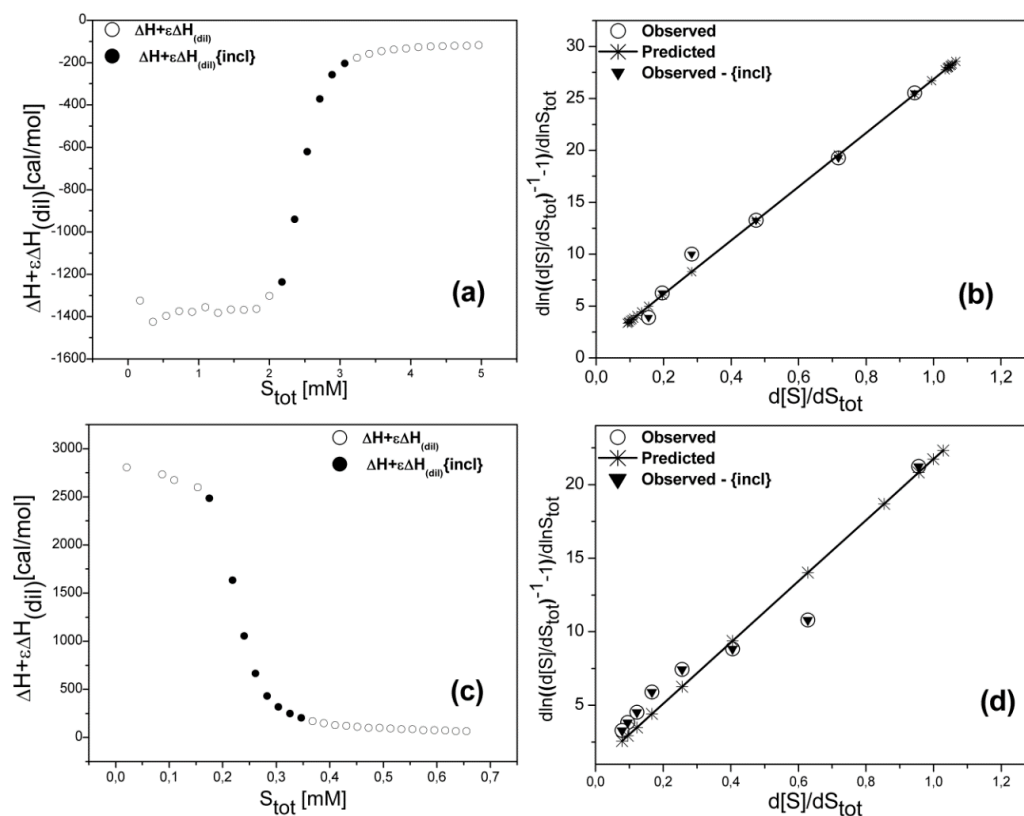


Fig. 8. a) Injections of 50 mM SB3-12 into water at 293.15 K in aliquots of 5 μ L, b) measurements shown in Fig. 8a) transformed according to Eq. 10, c) injections of 6 mM SB3-14 into water at 318.15 K in aliquots of 5 μ L, d) measurements shown in Fig. 8c) transformed according to Eq. 10. In all Figures grey and black points refer respectively to measurements included or excluded for further analysis.

Table 2. Micellar parameters for SB3-12 and SB3-14 calculated from ITC and DLS results.

SB3-12				
ITC			DLS	
T(K)	K (mM)	N_{agg}	D_h (nm)	N_{agg}
293.15	22600	28	7.80	282
298.15	21200	26	7.19	144
303.15	23700	21	7.49	106
308.15	23100	20	6.00	57
313.15	22900	18	6.15	44
318.15	21000	17	5.35	34
323.15	21300	/	5.11	19
SB3-14				
293.15	289000	/	6.12	131
298.15	220000	58	6.08	95
303.15	276000	51	5.95	70
308.15	268000	50	5.90	53
313.15	263000	36	5.89	41
318.15	244000	22	5.82	32
323.15	238000	20	5.59	25

Estimation of the aggregation number

Fig. 8a and 8c show typical ITC curves obtained for 50 mM SB3-12 at 293.15 K and 6 mM SB3-14 at 318.15 K, in water. Both experiments were performed with injections of 5 μ L aliquots. In Fig. 8b and 8d, the data are transformed according to Eq. 10. All estimated parameters for different temperatures are summarized in Table 2 together with the cmc and micellization constant calculated by Eq.11. The experimental data from Fig. 9 verifies that the theoretical methodology is reliable and effective.

Table 2 shows that aggregation numbers determined by ITC are lower than DLS values because they are determined at cmc whereas DLS method determines the aggregation number at higher concentrations, where the aggregation number is known to be high [38]. The DLS hydrodynamic diameter values approach from ITC at high temperatures because the hydration effect decreases which underlines its important contribution [16].

Sulfobetaines Interaction with Polymer

ITC results

The titration calorimetric curves for SB3-n surfactants in the presence and the absence of the PS-NPs polymer at different temperatures are presented in Fig. 9. Given the

pure surfactant ITC curves shown on Fig. 6 and their T_c s, it is clear that at concentrations beyond the corresponding cmcs, the PS-NPs/surfactant and pure surfactant curves are superposed. This means that the polymer does not influence micellization and thus unbound micelles exist in solution.

At concentrations near the corresponding cmcs, the ITC curves deviate from their pure counterparts for polymeric SB3-12 solutions and a clear shift of the cmc towards higher values occurs and seems to accentuate with temperature increase. For SB3-14 surfactants, the curves almost stick to each other for temperature $T = 293.15$ K but slightly deviate at higher temperature $T = 308.15$ K. In all these ITC curves, the curves separate at dilute concentration indicating surfactant/polymer interaction at concentrations below the cmc values, allowing the identification of a cac of 0.73 mM and 0.06 mM for SB3-12 at $T = 298.15$ K and SB3-14 at $T = 308.15$ K respectively. These ITC results show that at temperatures above T_c , the processes are endothermic emphasizing the occurrence of hydrophobic interaction between surfactants and polymer. At dilute concentrations below the micellization process, the polymer/surfactant complex transition for SB3-12 is less endothermic with a clear signal whereas for SB3-14 it is more endothermic with a weak signal.

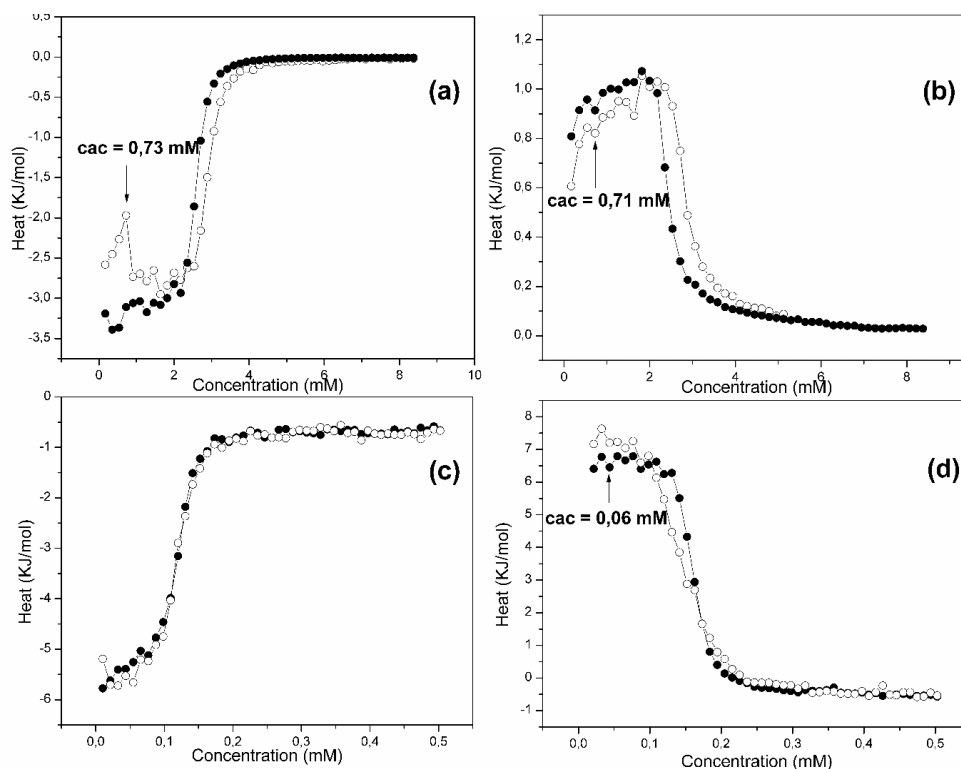


Fig. 9 Calorimetric titration curves for the addition of SB 3-12 (50 mM) at 298.15 K (a) and 308.15 K (b) to water (●) and to a 0.1 mM polymeric solution of PS-NPS (○). Calorimetric titration curves for the addition of SB 3-14 (3 mM) at 293.15 K (c) and 308.15 K (d) to water (●) and to a 0.1 mM polymeric solution of PS-NPS (○).

Accordingly, SB3-14 surfactants don't interact strongly with the polymer moieties and self-associate to form micelles when surfactant concentration increases.

Oppositely to the SB3-14 behavior, SB3-12 surfactants exhibit more attractive interaction with the polymer and enlargement of the polymer size is expected in the presence of such surfactant. For lower temperature case $T < T_c$, an obvious cooperative aggregation starts at a critical aggregation concentration, c_{ac} for SB3-12 at $T = 298.15$ K, meanwhile for SB3-14 no distinctive c_{ac} signal is recognized but a deviation of the curve exists. Here again the SB3-12 surfactant/polymer system must be the most disturbed and should exhibit size variation of the polymer nanoparticles at low temperatures. To explore this phenomenon, DLS measurements were conducted for such systems and results are shown on Fig. 10.

Dynamic light scattering results

The polymer hydrodynamic diameter (D_h) around the different ITC identified c_{ac} and c_{mc} for each

surfactant/polymer system are shown in Fig. 10 at temperatures below T_c corresponding to each surfactant. For SB3-12 surfactant, the polymer size D_h starts to increase around 0.75 mM from $D_h = 220$ nm to reach a maximum at a concentration equal to 1.2 mM with $D_h = 260$ nm and to finally decrease back to a constant size $D_h = 220$ nm beyond 2 mM. For SB3-14 a different behavior is obtained since an asymmetric peak is observed with an increase in D_h value around 0.03 mM then reaches a maximum at 0.4 mM to diminish as a plateau from 0.06 mM. Combined to the earlier conclusions drawn from ITC analysis, it is legitimate to claim that the c_{ac} for SB3-12 surfactant is situated at 0.75 mM and its c_{mc} in the neighborhood of 2 mM. These suggestions are in agreement with ITC measurements results ($c_{ac} = 0.70$ mM and $c_{mc} = 2.9$ mM). Similarly to SB3-12, ITC analysis of SB3-14 surfactant gives ($c_{ac} = 0.05$ mM and $c_{mc} = 0.12$ mM) values close to values determined by DLS ($c_{ac} = 0.03$ mM and $c_{mc} = 0.06$ mM).

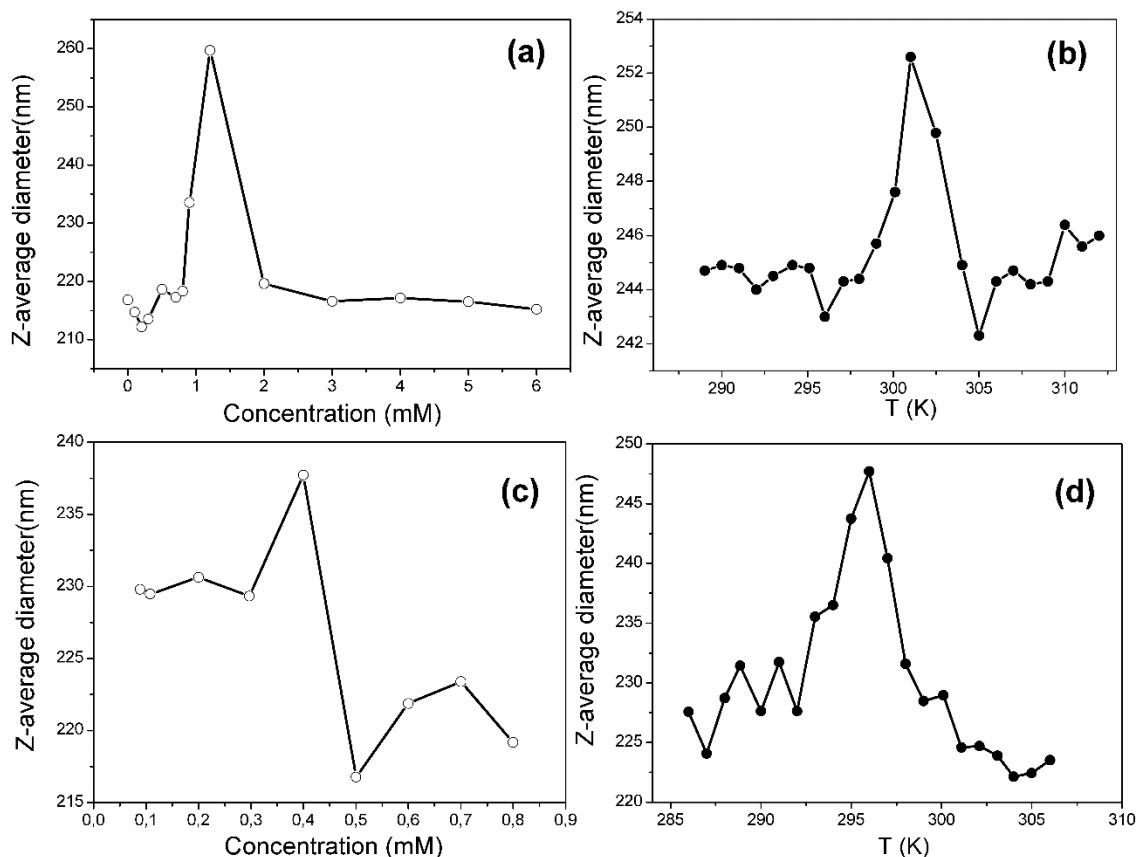


Fig. 10. Evolution of the hydrodynamic diameter of SB3-12 (a–b) (at 298.15 K) and SB3-14(c–d) (at 298.15 K) in a 0.1 mM polymeric solution of PS-NPS versus concentration (○) or temperature (●)

The thermal analysis of SB3-12/polymer and SB3-14/polymer systems by DLS above the deduced respective c_{mc} s allows the identification of two specific

temperatures ($T = 300.5$ K for SB3-12 and $T = 296.15$ K for SB3-14) which match with temperatures determined by ITC experiments.

Tensiometry results

Jones [39] and Lange [40] studied by tensiometry systems containing mixtures of the anionic surfactant sodium dodecyl sulphate (SDS) with poly(ethylene oxide) (PEO) or poly(vinyl pyrrolidone) (PVP), the surface tension behavior of surfactant polymer system is identifiable by three breaks historically designated B_1 , B_2 and B_3 , as shown in Fig. 11(b). The first break (B_1) corresponds to cac for the system recognized by the occurrence of a subtle plateau during the surface tension decrease regime. B_2 is the point where the bulk polymer is more or less saturated with free surfactants/micelles species and above which surface tension decreases again. This point is generally less defined than B_1 and the plateau B_1 - B_2 distance depends generally on polymer concentration on the bulk. Finally, the B_3 break which is identified as the beginning of a second more evident plateau in the surface tension at high surfactant concentration coincides to the cmc or the onset of formation of surfactant micelles formation in the bulk.

Compared to the classical surface tension variation of ionic surfactant, we can state from surface tensiometry measurements visible on Fig. 11 that the initial decrease in surface tension is caused by the adsorption of surfactant monomers with or without polymer. When the surfactant and polymer interact at the surface, adsorption occurs at much lower surfactant concentrations than occurs in the absence of polymer as is observed for SB3-12 surfactant curve. Nevertheless, for SB3-14 surfactant the initial decrease regime for surfactant solution with and without polymer are close to each other confirming the suggestion of notorious hydrophobic effect sites, ion-dipole associations between the dipole of the hydrophilic parts of the polymer and the ionic headgroups of the surfactant, or interactions between the hydrophobic regions of the polymer and the hydrocarbon chains as two types of weak interaction). Many works showed that B_3 is significantly higher for polymer/surfactant system than for pure surfactant case. This agrees with the observed results herein. From this surface tension study, it is clear that the cac values for SB3-12 and SB3-14 match well with 0.74 mM and 0.06 mM respectively.

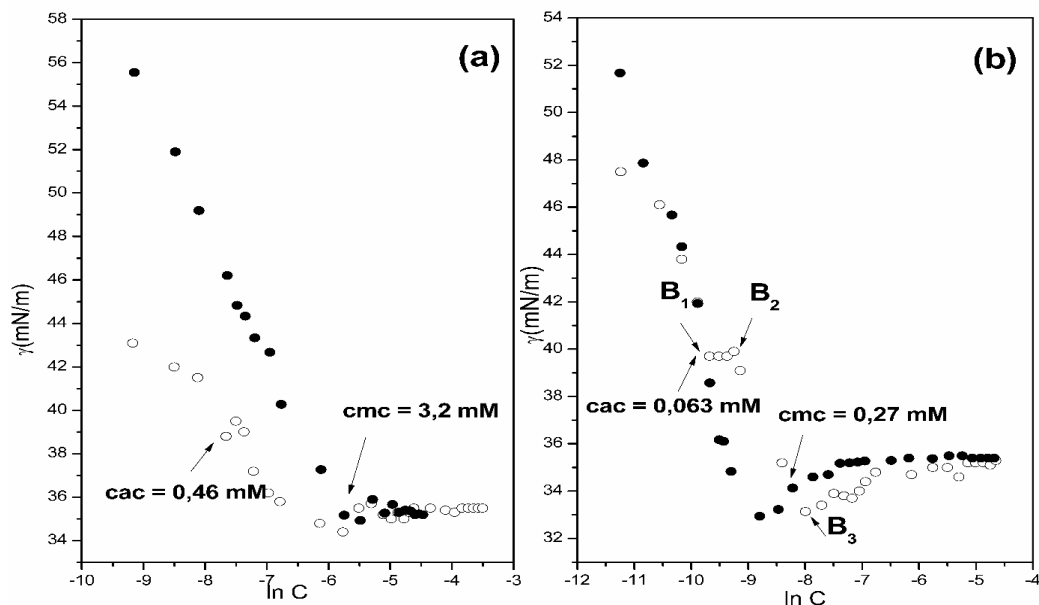


Fig. 11. Variation of surface tension of SB3-12 and SB3-14 against concentration at 298.15 K in the presence of PS-NPs.

5. Conclusions

This study aimed to explore the thermodynamics and physico-chemical properties associated with the micellization process of two zwitterionic surfactants, SB3-12 and SB3-14, belonging to the sulfobetaine family, both in the absence and presence of polystyrene nanoparticles. The characterization techniques employed, including tensiometry, dynamic light scattering (DLS), and isothermal titration calorimetry (ITC), indicated a

significant hydrophobic behavior of the SB3-14 surfactant. Consequently, SB3-14 exhibited a lower surface tension at the critical micelle concentration (cmc) compared to SB3-12, with a cmc value for SB3-12 being an order of magnitude higher ($cmc_{SB3-12} = 3.2$ mM via tensiometry, $cmc_{SB3-12} = 2.6$ mM via ITC, $cmc_{SB3-12} = 5$ mM via DLS) and $cmc_{SB3-14} = 0.28$ mM via tensiometry, $cmc_{SB3-14} = 0.24$ mM via ITC, $cmc_{SB3-14} = 0.4$ mM via DLS). The thermodynamic analysis conducted through ITC revealed

that hydrophobic interactions are present in the SB3-14 system even at low concentrations, with an entropic contribution observed at temperatures below the corresponding critical temperatures, aligning with the respective entropy-enthalpy compensation temperatures ($T_c=298.15$ K for SB3-14 and $T_c=306.15$ K for SB3-12). For the polymer/surfactant systems, the critical aggregation concentration (cac) was successfully determined for the SB3-12 surfactant (0.74 mM) using ITC, although the determination was less clear for SB3-14. Furthermore, surface tension measurements facilitated the identification of the cac for SB3-14 (0.06 mM) and highlighted its effective hydrophobic properties. The DLS method validated its capability to ascertain cmcs, critical temperatures, and aggregation numbers for the surfactants under study, as well as the cac, establishing it as a valuable tool for such investigations. The application of the methodology proposed by Olesen *et al.* [18] for extracting the aggregation number (N_{agg}) from ITC data demonstrated its effectiveness when applied to sulfobetaine surfactants, paving for the first time a new path for comparing N_{agg} derived from DLS.

Acknowledgment

The authors thank the DGRSDT and Mascara University, Algeria for technical support.

References

- [1] L. Zhao, J. Wang, X. Zhang, X. Guo, L. Chen, A. Zhang, K. Cao, J. Li, Experimental study on the evaluation of surfactant/polymer flooding for enhancing oil recovery in Kumkol Oil Field. *J Pet Explor Prod Technol.*, 13 (2023) 853–864.
- [2] P. Raffa, AA. Broekhuis, F. Picchioni, Polymeric surfactants for enhanced oil recovery: A review. *J Pet Sci Eng.*, 145 (2016) 723–733.
- [3] S. Llamas, E. Guzmán, F. Ortega, N. Baghdadli, C. Cazeneuve, RG. Rubio, GS. Luengo, Adsorption of polyelectrolytes and polyelectrolytes-surfactant mixtures at surfaces: A physico-chemical approach to a cosmetic challenge. *Adv Colloid Interface Sci.*, 222 (2015) 461–487.
- [4] M. Chen, NP. Hankins, Interaction among branched polyethylenimine (PEI), sodium dodecyl sulfate (SDS) and metal cations during copper recovery from water using polymer-surfactant aggregates. *J Water Process Eng.*, 34 (2020) 101170.
- [5] J.B. Stanislaus, Single Molecule Study of Polymer – Surfactant, Ph.D thesis, Bayreuth University, Bayreuth, Germany (2007).
- [6] C. Holmberg, S. Nilsson, LO. Sundelöf, Thermodynamic properties of surfactant/polymer/water systems with respect to clustering adsorption and intermolecular interaction as a function of temperature and polymer concentration. *Langmuir.*, 13(1997) 1392–1399.
- [7] RP. Gawade, SL. Chinke, PS. Alegaonkar, Polymer Science and Innovative Applications: Materials, Techniques, and Future Developments, India Prune (2020).
- [8] W. Loh, C. Brinatti, KC. Tam, Use of isothermal titration calorimetry to study surfactant aggregation in colloidal systems. *Biochim. Biophys. Acta - Gen. Subj.*, 1860 (2016) 999–1016.
- [9] DJF. Taylor, RK. Thomas, J. Penfold, Polymer/surfactant interactions at the air/water interface. *Adv Colloid Interface Sci.*, 132 (2007) 69–110.
- [10] S. Sharma, M. Kamil, Studies on the interaction between polymer and surfactant in aqueous solutions. *Indian J Chem Technol.*, 25 (2018) 294–299.
- [11] C. Brinatti, LB. Mello, W. Loh, Thermodynamic study of the micellization of zwitterionic surfactants and their interaction with polymers in water by isothermal titration calorimetry. *Langmuir.*, 30 (2014) 6002–6010.
- [12] SCF Mahler, Tso, J. Höring, S. Keller, C A. Brautigam, Fast and Robust Quantification of Detergent Micellization Thermodynamics from Isothermal Titration Calorimetry. *Anal Chem.* 92 (2020) 1154–1161.
- [13] K. Bouchemal, F. Agnely, A. Koffi, M. Djabourov, G. Ponchel, What can isothermal titration microcalorimetry experiments tell us about the self-organization of surfactants into micelles?. *J Mol Recognit.*, 23 (2010) 335–342.
- [14] M. Debolina, Use of isothermal titration calorimetry to study various systems. *Mater Today Proc.*, 23 (2020) 284–300.
- [15] KG. Kulikov, TV. Koshlan, Measurement of sizes of colloid particles using dynamic light scattering. *Tech. Phys.*, 60 (2015) 1758–1764.
- [16] A. Kadiri, T. Fergoug, KO. Sebakhy, Y. Bouhadda, R. Aribi, F. Yssaad, Z. Daikh, M. El Hariri El Nokab, PHM. Van Steenberge, Insights into the Characterization of the Self-Assembly of Different Types of Amphiphilic Molecules Using Dynamic Light Scattering. *ACS Omega.*, 8 (2023) 47714–47722.
- [17] Ferrer-Tasies, L., Cholesterol and Compressed CO₂: a Smart Molecular Building Block and Advantageous Solvent to Prepare Stable Self-assembled Colloidal Nanostructures, Ph.D thesis, Barcelona University, Barcelona, Spain (2016).
- [18] NE. Olesen, R. Holm, P. Westh, Determination of the aggregation number for micelles by isothermal titration calorimetry. *Thermochim Acta.*, 588 (2014) 28–37.
- [19] V. Domínguez-arca, J. Sabín, P. Taboada, L. García-río, G. Prieto, Micellization thermodynamic behavior of gemini cationic surfactants . Modeling its adsorption at air / water interface. *J Mol Liq.*, 308 (2020) 113100–113109.
- [20] DP. Cistola, JA. Hamilton, D. Jackson, DM. Small, Ionization and Phase Behavior of Fatty Acids in Water: Application of the Gibbs Phase Rule. *Biochemistry.*, 27 (1988) 1881–1888.
- [21] A. Taheri-Kafrani, AK. Bordbar, Energetics of micellization of sodium n-dodecyl sulfate at physiological conditions using isothermal titration calorimetry. *J Therm Anal Calorim.*, 98 (2009) 567–575.
- [22] NE. Olesen, P. Westh, R. Holm, Determination of thermodynamic potentials and the aggregation number for

- micelles with the mass-action model by isothermal titration calorimetry: A case study on bile salts. *J Colloid Interface Sci.*, 453 (2015) 79–89
- [23] J.N. Phillips, THE ENERGETICS OF MICELLE FORMATION. *Trans Faraday Soc.*, 51 (1955) 561-569.
- [24] C.J. Cheng, G.M. Qu, J.J. Wei, T. Yu, W. Ding, Thermodynamics of micellization of sulfobetaine surfactants in aqueous solution. *J Surfactants Deterg.*, 15 (2012) 757–763.
- [25] YA. Mirgorod, TA. Dolenko, Liquid Polyamorphous Transition and Self-Organization in Aqueous Solutions of Ionic Surfactants., *Langmuir.*, 31 (2015) 8535–8547.
- [26] B. Hammouda, Temperature Effect on the Nanostructure of SDS Micelles in Water. *J Res Natl Inst Stand Technol.*, 118 (2013) 151.
- [27] Profio P. Di, R. Germani, A. Fontana, V. Canale, Surface charge modulation of sulfobetaine micelles by interaction with different anions: A dynamic light scattering study. *J Mol Liq.*, 278 (2019) 650–657.
- [28] D. Asker, J. Weiss, D.J. McClements, Analysis of the interactions of a cationic surfactant (Lauric arginate) with an anionic biopolymer (Pectin): Isothermal titration calorimetry, light scattering, and microelectrophoresis., *Langmuir.*, 25 (2009) 116–122.
- [29] X. Wang, L. Yu, J. Jiao, H. Zhang, R. Wang, H. Chen, Aggregation behavior of COOH-functionalized imidazolium-based surface active ionic liquids in aqueous solution. *J Mol Liq.*, 173 (2012) 103–107.
- [30] K. Bijma, J.B.F.N. Engberts, M.J. Blandamer, P.M. Cullis, P.M. Last, K.D. Irlam, L.G. Soldi, Classification of calorimetric titration plots for alkyltrimethylammonium and alkylpyridinium cationic surfactants in aqueous solutions. *J Chem Soc Faraday Trans.*, 93 (1997) 1579–1584.
- [31] A. Kessler, B. Zeeb, B. Kranz, O. Menéndez-Aguirre, L. Fischer, J. Hinrichs, J. Weiss, Isothermal titration calorimetry as a tool to determine the thermodynamics of demicellization processes. *Rev.*, *J Rev Sci Instrum.*, 83 (2012) 105104–105109.
- [32] B. Šarac, M. Bešter-Rogač, Temperature and salt-induced micellization of dodecyltrimethylammonium chloride in aqueous solution: A thermodynamic study. *J Colloid Interface Sci.*, 338 (2009) 216–221.
- [33] M.M. Lopez, G.I. Makhatadze, Isothermal titration calorimetry. *Methods Mol Biol.*, 173 (2002) 121–126.
- [34] E. Sikorska, D. Wyrzykowski, K. Szutkowski, K. Greber, E.A. Lubecka, I. Zhukov, Thermodynamics, size, and dynamics of zwitterionic dodecylphosphocholine and anionic sodium dodecyl sulfate mixed micelles., *J Therm Anal Calorim.*, 123 (2016) 511–523.
- [35] G. Sugihara, T.Y. Nakano, S.B. Sulthana, A.K. Rakshit, Enthalpy-Entropy Compensation Rule and the Compensation Temperature Observed in Micelle Formation of Different Surfactants in Water. What is the so-called Compensation Temperature?. *J Oleo Sci.*, 50 (2001) 29–39.
- [36] R. Aribi, C. Zemat, T. Fergoug, Y. Bouhadda, M. Dadouch, F. Yssaad, A. Kadiri, F.Z. Chater, Micellar properties and partial phase diagram of cetyltrimethylammonium bromide and cetylpyridinium chloride in vicinity of Krafft point from conductometry and dynamic light scattering measurements. *J. Chem. Lett.*, 7 (2024) 773-785.
- [37] Y. Zheng, X. Lu, L. Lai, L. Yu, H. Zheng, C. Dai, The micelle thermodynamics and mixed properties of sulfobetaine-type zwitterionic Gemini surfactant with nonionic and anionic surfactants. *J Mol Liq.*, 299 (2020) 112108.
- [38] A.I. Rusanov, Micellization theory based on the law of mass action with a variable aggregation number. *Colloid J.*, 79 (2017) 654–660.
- [39] M.N. Jones, The interaction of sodium dodecyl sulfate with polyethylene oxide. *J Colloid Interface Sci.*, 23 (1967) 36–42.
- [40] Lange, H., Wechselwirkung zwischen Natriumalkylsulfaten und Polyvinylpyrrolidon in wäßrigen Lösungen., *Kolloid-Zeitschrift Zeitschrift für Polym.*, 243 (1971) 101–109.